# Through-Hole Drilling of Flame-Retardant Polyester-Based Films Using a Short-Pulse $CO_2$ Laser

Kazuyuki Uno*

*Integrated Graduate School of Medicine, Engineering, and Agricultural Sciences, University of Yamanashi*
**Corresponding author's e-mail: kuno@yamanashi.ac.jp*

Through-hole drilling of a 200-μm-thick flame-retardant polyester-based film was investigated using a short-pulse $CO_2$ laser with a pulse width of 304 ns. Percussion drilling was performed at a repetition rate of 200 Hz and a fluence of 10.7 J/cm$^2$ per pulse. Two irradiation methods were examined. One was conventional continuous irradiation, referred to as Continuous Irradiation in this paper. The other was a method referred to as Divided Pulse Train Irradiation. In this method, a sequence of laser pulses (a pulse train) is followed by a certain time interval before the next pulse train is delivered. The minimum number of pulses required to form a through-hole was 75 in Continuous Irradiation, whereas only 4 pulses were sufficient in Divided Pulse Train Irradiation. In this case, 2 pulses were applied in the first set and 2 in the second set, with a time interval of 0.5 ms or longer. Discoloration was observed around the hole in Continuous Irradiation but was absent in Divided Pulse Train Irradiation, suggesting that thermal effects were effectively suppressed in the latter.
DOI: 10.2961/ilmn.2026.01.2002
**Keywords:** through-hole, drilling, polymer film, flame-retardant polyester, $CO_2$ laser

## 1. Introduction

Functional polymer resins can be endowed with various properties—such as heat resistance, mechanical strength, chemical resistance, electrical conductivity, hydrophilicity/hydrophobicity, and biocompatibility—through compositional adjustment and the incorporation of functional additives. Owing to these tunable characteristics, they have become indispensable materials across a wide range of industrial fields, including aerospace and transportation equipment, electronics, medical devices, and consumer goods. In the fabrication of components and structures using these polymer materials, there is a growing demand for high-speed, high-precision, and high-quality processing, as well as energy-efficient and cost-effective production methods. In recent years, the development of various functional polymers has been accompanied by significant advances in laser systems and processing technologies. To make effective use of these advancements, it is essential to optimize processing parameters, which remains a key challenge [1-12].

Many polymer resins efficiently absorb infrared radiation, particularly in the wavelength range of 9–11 μm. Laser sources capable of emitting in this spectral region include $CO_2$ lasers, quantum cascade lasers (QCLs), lead-salt semiconductor lasers [13-23]. Among these, $CO_2$ lasers are effective tool for polymer processing due to its capability to deliver high pulse energies ranging from several tens of millijoules to several joules, high average powers from several tens of watts to several tens of kilowatts, and its ability to operate in various modes such as short pulses (tens to hundreds of nanoseconds), long pulses (tens of microseconds to several milliseconds), and continuous-wave (CW) output [13-20].

In $CO_2$ laser processing, short-pulse irradiation induces thermal processing accompanied by ablation, whereas long-pulse and continuous-wave (CW) irradiation predominantly result in purely thermal effects. Due to the thermal nature of these processes, undesirable thermal effects such as carbonization, melting, discoloration, and cracking may occur depending on the irradiation conditions, irradiation method, and the thermal properties of the material [1-7]. Therefore, the suppression of such thermal effects is a critical challenge in $CO_2$ laser processing of polymers.

To address this challenge, it is essential to optimize laser parameters such as pulse shape, beam profile, repetition rate, and fluence per pulse. In addition, process parameters including the number of irradiation pulses and the pulse overlap rate must be appropriately selected, along with the flow rate of assist gas, which is used to promote or suppress oxidation reactions and to remove debris from the processing area. Water-assisted processing, which serves to cool the workpiece and remove debris, is also a commonly employed technique; however, because the wavelength of $CO_2$ lasers is strongly absorbed by water, alternative approaches—such as the use of nanoliquids—have been proposed [24-26]. Furthermore, thermal properties of the target material, such as melting point, thermal expansion coefficient, thermal conductivity, and thermal diffusivity, are also important factors to consider for effective control of thermal effects.

Previous studies by the authors have demonstrated that crack-free hole drilling using short-pulse $CO_2$ lasers not only in synthetic fused silica glass, which has a low thermal expansion coefficient ($5.5 \times 10^{-7}$ /K) and a high melting point (1600 °C), but also in crown glass ($100 \times 10^{-7}$ /K, 724 °C), soda-lime glass ($87 \times 10^{-7}$ /K, 740 °C), and borosilicate glass ($33 \times 10^{-7}$ /K, 820 °C), which are characterized by higher thermal expansion coefficients and lower melting points [27]. Furthermore, they have reported that the taper angle of the machined geometry can be controlled by optimizing the

irradiation conditions [28]. These results suggest that precise control over the temperature distribution of the workpiece—enabled by appropriate $CO_2$ laser parameter adjustments—can allow for accurate control of both processing quality and geometry.

In this study, hole drilling was performed on a flame-retardant polyester-based film, which contains a flame-retardant layer that promotes char formation during combustion, suppressing oxygen diffusion and reducing flame spread [29-31], using a short-pulse $CO_2$ laser. The challenges associated with conventional polymer processing by continuous laser pulse irradiation—namely, the expansion of thermal effects and degradation of processing quality—were elucidated. Furthermore, irradiation methods to overcome these challenges were investigated, and processing conditions aimed at improving processing efficiency and reducing thermal influence were explored.

## 2. Experimental setup

Figure 1 shows a schematic diagram of the experimental setup. A custom-developed longitudinally excited (LE) $CO_2$ laser was used, operating at a wavelength of 10.6 μm with a repetition rate of 200 Hz [13,14,27,28]. Fig. 2 shows the pulse shape and beam profile of the laser output. The pulse

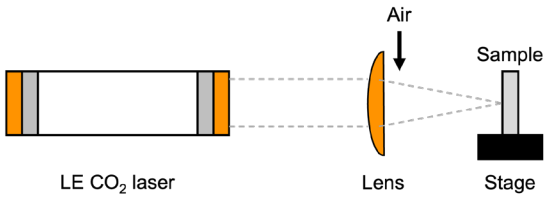


**Fig. 1** Experimental setup.

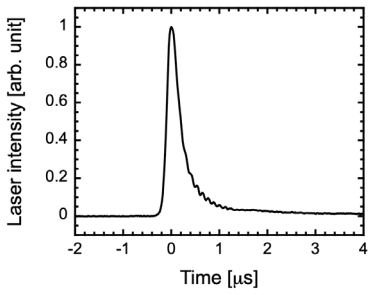


(a)

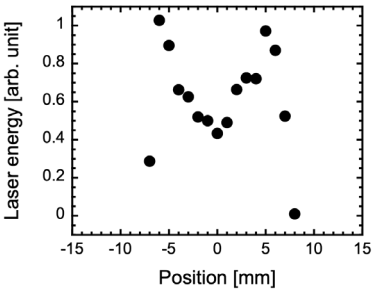


(b)

**Fig. 2** Laser pulse shape and beam profile.
(a) Laser pulse. (b) Laser beam.

shape was recorded using a photodetector (Hamamatsu Photonics, P13894-011MA), yielding a pulse width of 304 ns. The spatial intensity distribution of the beam was measured using a slit and an energy meter (Gentec, QE50LP-S-MB-D0); it exhibited a doughnut-shaped profile with a diameter of 14.9 mm. The beam was focused by a lens with a focal length of 12.7 mm. The sample was placed so that its surface was aligned with the focal plane of the lens. The resulting spot diameter (i.e., the irradiation diameter) was 198 μm, and the fluence per pulse was 10.7 J/cm$^2$.

The sample used in this study was a flame-retardant polyester-based film (Dialamy, Mitsubishi Chemical) with a thickness of 200 μm. The flame-retardant polyester-based film had a three-layer structure, consisting of a 50-μm-thick flame-retardant layer sandwiched between two 75-μm-thick polyester layers. To protect the lens from fumes and dust, a stream of air was introduced; however, this airflow was not directed onto the sample surface. Fumes and particulates generated during laser processing were extracted by an activated carbon deodorization unit.

Two irradiation methods were investigated in this study, as illustrated in Fig. 3. One was conventional continuous irradiation, referred to as Continuous Irradiation in this paper. The other was a method referred to as Divided Pulse Train Irradiation in this paper. In Divided Pulse Train Irradiation, a sequence of laser pulses (a pulse train) is followed by a certain time interval before the next pulse train is delivered. Since the laser pulses used in this study are nanosecond pulses, the term Divided Pulse Train Irradiation is adopted to distinguish it from burst-mode irradiation, as typically employed with femtosecond lasers, which operates on a much shorter temporal scale [12,32,33].

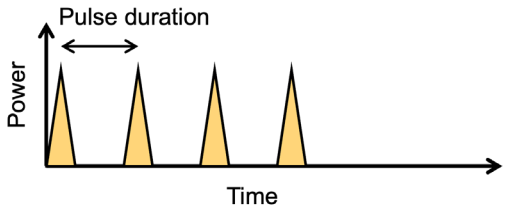


(a)

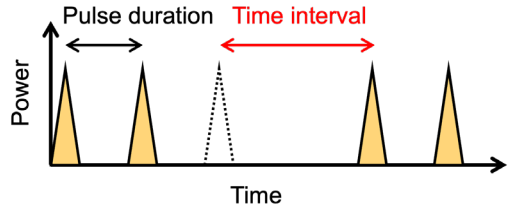


(b)

**Fig. 3** Continuous Irradiation and Divided Pulse Train Irradiation.
(a) Continuous Irradiation. (b) Divided Pulse Train Irradiation.

## 3. Results and discussion

Figure 4 shows images of the sample surface after Continuous Irradiation at a repetition rate of 200 Hz. To form a through-hole in the 200-μm-thick flame-retardant polyester-

| Number of pulses | 1 | 2 | 5 | 10 | 30 | 75 | 100 | 200 |
|---|---|---|---|---|---|---|---|---|
| Total irradiation fluence [J/cm$^2$] | 10.7 | 21.4 | 53.5 | 107 | 321 | 803 | 1070 | 2140 |
| FR polyester film (200 μm) | 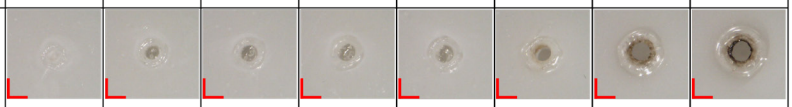 | | | | | | | |
| Hole formation | No | No | No | No | No | Yes | Yes | Yes |
| Discoloration | No | No | Yes | Yes | Yes | Yes | Yes | Yes |
| Polyester layer (75 μm) | 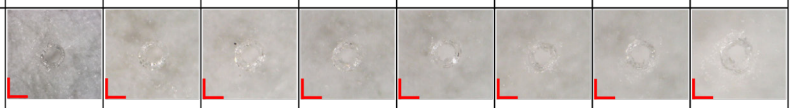 | | | | | | | |
| Hole formation | Yes | Yes | Yes | Yes | Yes | Yes | Yes | Yes |
| Discoloration | No | No | No | No | No | No | No | No |
| FR layer + Polyester layer (125 μm) | 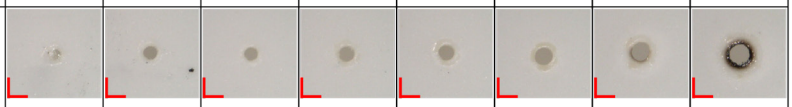 | | | | | | | |
| Hole formation | No | Yes | Yes | Yes | Yes | Yes | Yes | Yes |
| Discoloration | No | No | Yes | Yes | Yes | Yes | Yes | Yes |

**Fig. 4** Sample surface images and summary of results under Continuous Irradiation. The red scale bar indicates 200 μm.

based film, more than 75 pulses were required at 200 Hz, corresponding to a processing time of 350 ms. At a repetition rate of 100 Hz, 20 pulses (200 ms) were required, and at 50 Hz, 10 pulses (also 200 ms) were sufficient. Discoloration or carbonization was observed around the resulting through-holes. These results were highly reproducible, with through-hole formation and discoloration consistently observed at the same pulse numbers under identical conditions.

The flame-retardant polyester-based film used in the experiment had a three-layer structure, consisting of a 50-μm-thick flame-retardant layer sandwiched between two 75-μm-thick polyester layers. The surface polyester layers could be peeled off. In the case of the 75-μm-thick polyester layer alone, a single pulse was sufficient to form a through-hole, and even after 200 pulses at a repetition rate of 200 Hz, no discoloration was observed.

For a structure comprising a 50-μm-thick flame-retardant layer and a 75-μm-thick polyester layer, when laser pulses were irradiated from the flame-retardant side at a repetition rate of 200 Hz, a through-hole was formed with just 2 pulses, but discoloration occurred with 5 or more pulses. These results indicate that the discoloration or carbonization observed during through-hole formation in the 200-μm-thick flame-retardant polyester-based film originated from the flame-retardant layer, likely due to the thermal decomposition of the flame-retardant additives [29-31].

Additionally, in the 200-μm-thick flame-retardant polyester-based film with a three-layer structure, molten material flowed into the hole and blocked it, even after a through-hole had initially been formed during Continuous Irradiation. As a result, the number of pulses required for through-hole formation increased. This was demonstrated by an experiment in which a photodetector was placed behind the film to monitor laser pulses that passed through the hole. Even in samples where a through-hole was ultimately not formed, the detector responded and recorded laser pulses identical to the incident ones, indicating that the laser passed through the hole.

Figure 5 shows images of the sample surface after Divided Pulse Train Irradiation with a time interval of 10 s. A through-hole was formed with a total of 4 pulses—2 pulses irradiated initially, followed by another 2 pulses after a 10-second interval. No discoloration was observed around the through-hole.

Figure 6 shows sample surface images obtained by Divided Pulse Train Irradiation, in which 2 pulses were irradiated first, followed by another 2 pulses after a variable time interval. No through-holes were formed when the time interval was shorter than 0.5 ms. However, when the time interval was 0.5 ms or longer, through-holes were formed. No discoloration was observed around the through-hole. The same experiments were repeated several times under identical conditions, and the results were highly reproducible. Throu-

| No. of 1st pulses | 1 | 1 | 2 | 2 | 2 |
|---|---|---|---|---|---|
| No. of 2nd pulses | 2 | 5 | 1 | 2 | 5 |
| Total irradiation fluence [J/cm$^2$] | 32.1 | 64.2 | 32.1 | 42.8 | 74.9 |
| FR polyester film (200 μm) |  | | | | |
| Hole formation | No | No | No | Yes | Yes |
| Discoloration | No | No | No | No | No |

**Fig. 5** Sample surface images and summary of results under Divided Pulse Train Irradiation with a time interval of 10 s. The red scale bar indicates 200 μm.

| Time interval [ms] | 0 | 0.1 | 0.2 | 0.5 | 1.0 |
|---|---|---|---|---|---|
| FR polyester film (200 μm) | 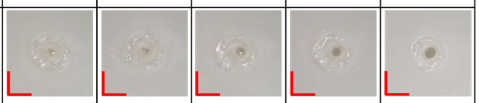 | | | | |
| Hole formation | No | No | No | Yes | Yes |
| Discoloration | No | No | No | No | No |

**Fig. 6** Sample surface images and summary of results under Divided Pulse Train Irradiation with 2 pulses in the first set and 2 pulses in the second set. The red scale bar indicates 200 μm.

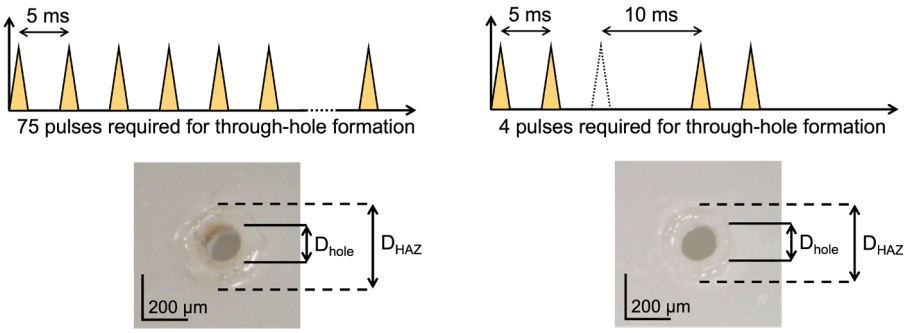


| Number of pulses | 75 pulses |
|---|---|
| Total time | 370 ms |
| Total irradiation fluence | 803 J/cm$^2$ |
| Discoloration | Yes |
| Surface hole diameter ($D_{hole}$) | 137 μm |
| Surface HAZ diameter ($D_{HAZ}$) | 370 μm |

(a)

| Number of pulses | 4 pulses |
|---|---|
| Total time | 25 ms |
| Total irradiation fluence | 42.8 J/cm$^2$ |
| Discoloration | No |
| Surface hole diameter ($D_{hole}$) | 149 μm |
| Surface HAZ diameter ($D_{HAZ}$) | 327 μm |

(b)

**Fig. 7** Comparison of processing results between Continuous Irradiation and Divided Pulse Train Irradiation under the minimum number of pulses required for through-hole formation.
(a) Continuous Irradiation with 75 pulses. (b) Divided Pulse Train Irradiation with 2 pulses in the first set and 2 pulses in the second set, with a time interval of 10 ms.

gh-holes were consistently formed at the same pulse timing as shown in Figs. 5 and 6.

Figure 7 summarizes a comparison between Continuous Irradiation and Divided Pulse Train Irradiation in terms of the minimum number of pulses required to achieve through-hole formation under the conditions used in this study. Compared with Continuous Irradiation, Divided Pulse Train Irradiation enabled through-hole formation with a significantly lower number of pulses, shorter processing time, and reduced total irradiation fluence. While discoloration occurred around the through-hole during Continuous Irradiation, no such discoloration was observed in the case of Divided Pulse Train Irradiation, suggesting that thermal effects were effectively suppressed. The hole diameter ($D_{hole}$) and the diameter of the heat-affected zone ($D_{HAZ}$, defined here as the melted region) were found to be nearly the same between Continuous Irradiation and Divided Pulse Train Irradiation.

Figure 8 shows the dependence of the $D_{hole}/D_{laser}$ ratio and $D_{HAZ}/D_{laser}$ ratio on the time interval for Divided Pulse Train Irradiation with 2 pulses in both the first and second sets. Since both the hole diameter $D_{hole}$ and HAZ diameter $D_{HAZ}$ depend on the laser irradiation diameter $D_{laser}$, the ratios $D_{hole}/D_{laser}$ and $D_{HAZ}/D_{laser}$ were used for evaluation. The $D_{hole}/D_{laser}$ ratio increased with time interval up to 10 ms and then saturated at approximately 69.0% for intervals longer than 10 ms. In contrast, the $D_{HAZ}/D_{laser}$ ratio decreased with increasing time interval up to 10 ms and then remained constant at approximately 145% for longer intervals. High reproducibility was obtained, with the variation in the measured ratios within approximately 8.4%.

## 4. Conclusion

In this study, hole drilling of a 200-μm-thick flame-retardant polyester-based film was investigated using a short-pulse $CO_2$ laser with a pulse width of 304 ns. Percussion irradiation was performed at a repetition rate of 200 Hz and a fluence of 10.7 J/cm$^2$ per pulse. The minimum number of pulses required to form a through-hole was 75 for Continuous Irradiation and only 4 for Divided Pulse Train Irradiation, in which 2 pulses were applied in the first set and 2 pulses in the second set, with a time interval of 0.5 ms or longer. Under Continuous Irradiation, even when a through-hole was formed, the molten material flowed into the hole and reblocked it. In contrast, such reblocking was avoided in Divided Pulse Train Irradiation. Furthermore, compared to Co-

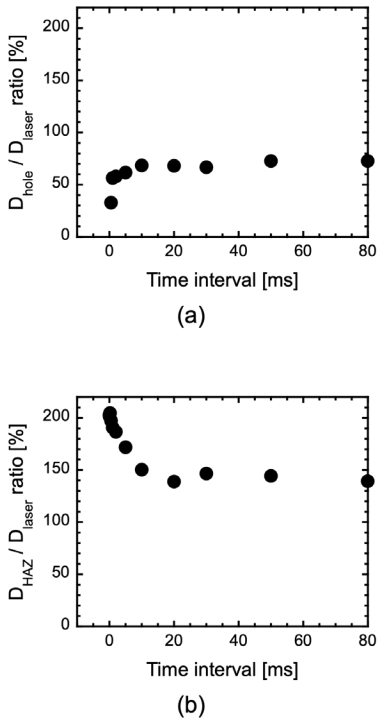


**Fig. 8** Dependence of $D_{hole}/D_{laser}$ and $D_{HAZ}/D_{laser}$ ratios on the time interval for Divided Pulse Train Irradiation with 2 pulses in each set.
(a) $D_{hole}/D_{laser}$ ratio. (b) $D_{HAZ}/D_{laser}$ ratio.

ntinuous Irradiation, the Divided Pulse Train Irradiation enabled through-hole formation with a significantly smaller number of pulses, shorter processing time, and lower total irradiation fluence. Discoloration was observed around the hole in Continuous Irradiation but was absent in Divided Pulse Train Irradiation, suggesting that thermal effects were effectively suppressed in the latter. Further investigations are needed to determine whether similar effects can be achieved in other materials.

**Acknowledgments**
The author would like to thank Mr. Daikichi Miyagawa, a former member of the research group at University of Yamanashi, for his contributions to this research. The author also would like to thank Seidensha Electronics CO., LTD of Japan for their support.

**References**

[1] A. Anjum, M. A. Ali, A. A. Shaikh, and S. S. Akhtar: Opt. Laser Technol., 176, (2024) 110860.
[2] C. Palanisamy and N. Ezhumalai: AIP Conf. Proc., 3240, (2024) 020003.
[3] J. L. Okello, A. M. R. F. El-Bab, M. Yoshino, and H. A. El-Hofy: Multiscale Multidiscip. Model. Exp. Des., 7, (2024) 617.
[4] C. Palanisamy, M. Efzan, and C. C. Wen: MethodsX, 10, (2023) 102125.
[5] O. Der, G. Basar, and M. Ordu: J. Mater. Mechatron., A 4, (2023) 459.
[6] A. E. Abdulwahab, K. A. Hubeatir, and K. I. Imhan: J. Eng. Appl. Sci., 69, (2022) 98.
[7] D. E. Ghoochani, F. R. Biglari, and H. Pazokian: Opt. Laser Technol., 139, (2021) 106879.
[8] L. Vysin, J. Chalupsky, L. A. Rush, L. Fekete, J. Bulicka, P. Mojzes, Z. Kuglerova, J. Krasa, L. Juha, J. J. Rocca, and C. S. Menoni: Polym. Degrad. Stab., 236, (2025) 111298.
[9] J. Xu, G. Zhang, Y. Rong, and Y. Huang: Opt. Laser Technol., 167, (2023) 109769.
[10] G. Ye, W. Wang, D. Fan, and P. He: Appl. Surf. Sci., 538, (2021) 148117.
[11] K. Moghadasi, K. F. Tamrin, N. A. Sheikh, and M. Jawaid: Int. J. Adv. Manuf. Technol., 117, (2021) 523.
[12] E. Kazukauskas, S. Butkus, P. Tokarski, V. Junkna, M. Barkauskas, and V. Sirutkaitis: Micromachines, 11, (2020) 1093.
[13] R. Okawa, K. Uno, S. Watarai, and Y. Kodama: Appl. Phys., B 131, (2025) 43.
[14] K. Uno, K. Yanai, S. Watarai, Y. Kodama, K. Yoneya, and T. Jitsuno: Opt. Laser Technol., 152, (2022) 108174.
[15] J. Ye, Z. Zhu, Y. Lu, J. Bai, X. Su, R. Tan, and Y. Zheng: Opt. Eng., 62, (2023) 056102.
[16] B. A. Kozlov and A. Y. Payurov: Proc. SPIE, Vol. 11322, (2019) 113220F.
[17] A. A. Ionin, I. O. Kinyaevskiy, Y. M. Klimavhev, A. A. Kotkov, A. Y. Kozlov, and A. M. Sagitova: Infrared Phys. Technol., 105, (2020) 103250.
[18] Y. Tadokoro, T. Tamamoto, and J. Nishimae: Proc. SPIE, Vol. 11266, (2020) 1126613.
[19] Y. S. Lee, H. J. Chung, J. H. Joung, E. J. Kim, and H. J. Kim: Opt. Laser Technol., 36, (2004) 57.
[20] S. J. Park and W. Y. Kim: Opt. Laser Technol., 42, (2010) 269.
[21] T. Edamura, T. Dougakiuchi, A. Sugiyama, and N. Akikusa: Photonics Rev., 2023, (2023) 230202.
[22] M. Joharifar, H. Dely, X. Pang, R. Schatz, D. Gacemi, T. Salgals, A. Udalcovs, Y. T. Sun, Y. Fan, L. Zhang, E. Rodriguez, S. Spolitis, V. Bobrovs, X. Yu, S. Lourdudoss, S. Popov, A. Vasanelli, O. Ozolins, and C. Sirtori: J. Light. Technol., 41, (2023) 1087.
[23] M. Tacke: Philos. Trans. Math. Phys. Eng. Sci., 359, (2001) 547.
[24] J. Wei, S. Yuan, S. Yang, M. Gao, Y. Fu, T. Hu, X. Li, X. Fan, and W. Zhang: Surf. Coat. Technol., 484, (2024) 130791.
[25] A. Kruusing: Opt. Lasers Eng., 41, (2004) 329.
[26] M. N. Mahdi, A. Issa, H. S. Hasan, A. R. Al-Hamaoy, and M. M. Hanon: Photonics, 10, (2023) 89.
[27] K. Uno, Y. Kodama, and K. Yoneya: J. Eng. Appl. Sci., 70, (2023) 137.
[28] M. E. Rahaman and K. Uno: Laser Phys., 33, (2023) 096004.
[29] A. Bifulco, C. Imparato, A. Aronne, and G. Malucelli: J. Sol-Gel Sci. Technol., 115 (2025) 226.
[30] M. S. Myrad, A. K. Hamzat, E. Asmatulu, and R. Asmatulu: Adv. Compos. Hybrid Mater., 8 (2025) 31.
[31] I. M. D. C. Cordeiro, T. B. Y. Chen, A. C. Y. Yuen, Q. Chen, W. Yang, C. Wang, W. Wang, Q. N. Chan, J. Zhang, W. Yang, and G. H. Yeoh: Chem. Eng. J., 480 (2024) 148169.
[32] M. Park, Y. Gu, X. Mao, C. P. Grigoropoulos, and V. Zorba: Sci. Adv., 9, (2023) eadf6397.
[33] E. Audouard and E. Mottay: Int. J. Extreme Manuf., 5, (2023) 015003.

(Received: June 11, 2025, Accepted: November 24, 2025)